S8-3

Progress in Turbulence Optimization Research for Stellarator Plasmas

Josefine H E Proll, Pavlos Xanthopoulos[2], Harry Mynick[3], Sam A Lazerson[3]

[1]*Eindhoven University of Technology, Eindhoven, The Netherlands,* [2]*Max Planck Institute for Plasma Physics, Greifswald, Germany,* [3]*Princeton Plasma Physics Laboratory, Princeton University, Princeton, USA*

Optimizing stellarators for turbulent transport is one of the next steps before a successful stellarator reactor can be built. Due to the high computational costs, including nonlinear simulations in the optimization routine is not feasible. So-called proxies are therefore sought – expressions, usually motivated by analytical theory, that allow estimates of the relative turbulent transport levels based on inputs from magnetic geometry. Both for ion-temperature-gradient modes as well as trapped-electron modes proxies have already been found and successfully applied. In the future, including also the physics of nonlinear saturation of turbulence might increase the success of turbulence optimization even more.

1. The Need for Turbulence Optimization

With the advent of neoclassically optimized stellarators like Wendelstein 7-X, turbulent transport is expected to be the dominant transport channel in large parts of the plasma. In the first campaigns by Wendelstein 7-X, the observed transport could in fact not fully be explained by neoclassical transport, thus indicating that turbulent transport plays a significant role [1].

In recent years, fully nonlinear simulations of turbulence driven by microinstabilities have become available for stellarator geometry. They reveal very interesting differences between the different geometries, in particular with regards to the transport levels [2]. An effect of the geometry on the microinstabilities that drive turbulence was already known from linear simulations – for example, Wendelstein 7-X had been observed to have lower growth rates of both ion-temperature-gradient modes (ITG) as well as trapped-electron modes (TEM) [3] than the HSX stellarator or a typical tokamak. In the nonlinear simulations, this behavior is retained, though the difference between HSX and Wendelstein 7-X is less pronounced. Nevertheless, the evident connection between magnetic field geometry and turbulence levels encourages optimization attempts also for turbulent transport.

While using the nonlinear turbulent heat flux of a certain magnetic configuration would be the most trustworthy measure of quality with respect to turbulent transport, it is not very feasible. The main reason for this are the prohibitively high amounts of computing time required – for example, a typical well-resolved simulation of TEM turbulence in stellarator geometry requires millions of CPUh.

To enable large scans over the vast space of 3D configurations we therefore need simplified, easy-to-compute expressions that serve as proxies for the turbulent transport.

In the remainder of this paper we therefore present the ideas behind proxies for both major electrostatic instabilities, ITGs and TEMs and the first successes in turbulence optimization. Finally, we provide an outlook for future turbulence optimization work.

2. Optimizing for Reduced ITG and TEM Turbulence Using STELLOPT

2.1 *Optimizing for reduced ITG turbulence*

As one of the first successes in terms of turbulence optimization, a reduction of ITG turbulence has been achieved by Mynick, Xanthopoulos and Pomphrey [4-7]. The idea behind this proxy is to reduce the drive for the ITG mode by reducing the unfavorable ("bad") curvature κ^{-}_{r} of the magnetic field lines as well as increasing the distance between adjacent flux surfaces, expressed by the inverse of the radial covariant metric element g^{rr}. The proxy to be minimized for ITG optimization is thus $\chi^2_{ITG} = \kappa^{-}_{r} (g^{rr})^2$, where squaring the metric element has been found to be most efficient for optimization.

This proxy has been implemented in the STELLOPT code [8] – a code designed to optimize 3D MHD equilibria with respect to a multitude of goals included in one cost function. For example, STELLOPT can simultaneously optimize for not only turbulent but also neoclassical transport – the latter is represented by including the neoclassical effective ripple as a proxy. The variation of the equilibria is achieved by treating the boundary harmonics of the equilibria as free parameters. The minimum of the cost function is then found by employing either steepest-decent methods like a modified Levenberg-Marquardt or stochastic algorithms like differential evolution. An example of a successful STELLOPT run is shown in Fig. 1. During the optimization process, the proxy value for ITGs, χ^2_{ITG}, is generally going down. For this optimization, an additional constraint was also put on the neoclassical transport, which was increasing for higher equilibrium indices (not shown here). The equilibrium thus chosen as the optimum and titled MPX was thus not completely at the minimum of χ^2_{ITG}. It is predicted to have lower ITG turbulence than W7-X though.

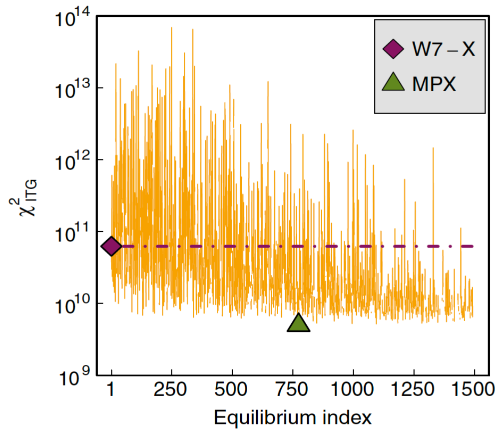

Fig.1. Values of the ITG proxy value for the different equilibria of the STELLOPT run which resulted in finding the MPX configuration. MPX clearly has a much lower ITG proxy than W7-X. Configurations with even lower ITG proxy value (higher equilibrium indexes) were not chosen because of their higher neoclassical transport (not shown here). Reprinted from [7]

The success of the optimization can be checked by running nonlinear simulations. In [7] it was shown that the nonlinear ITG heat flux in MPX is indeed lower than W7-X for a range of temperature gradients and the optimization was thus successful.

2.2. Optimizing for reduced TEM turbulence

Also for TEM turbulence, a proxy motivated by analytical theory can be defined. The energy transfer between kinetic electrons and the modes has been found to be proportional to the bounce-averaged curvature $\overline{\omega}_d$ of a given particle with pitch angle λ integrated over all pitch angles [9,10]. More particles having negative ("bad") bounce-averaged curvature will result in more energy being transferred to the modes. The proxy to be minimized is thus the negative averaged curvature.

$$Q = -\int_{1/B_{max}}^{1/B_{min}} \overline{\omega}_d(\lambda)\mathrm{d}\lambda$$

A successful optimization starting from the HSX stellarator which resulted in a reduction of the nonlinear TEM heat flux has been demonstrated in [11].

3. Outlook

As the geometry changes in the course of the optimization, not only the linear drive but also the nonlinear saturation mechanisms change. Proxies which account for the nonlinear as well as linear effects could provide a large advance in their generality.

In recent years, some progress has been made towards understanding the dynamics of different saturation mechanisms. Nunami *et al.* have obtained a model for zonal flows for LHD geometry [12], Plunk *et al.* found and explanation why zonal flows are stronger in W7-X geometry than in HSX geometry [13] and Hegna *et al.* showed how understanding the coupling of the unstable modes to damped modes helps in understanding saturation in HSX geometry [14]. Developing these ideas further and extending them to different modes and arbitrary geometry will allow for a more faithful modelling of turbulent transport and more powerful optimization routines.

References

[1] A. Dinklage *et al.*, Nature Physics **14** (2018) 85.
[2] J.H.E. Proll *et al.,* to be published
[3] J.H.E. Proll *et al.*, Phys. Plasmas **20** (2013) 122506.
[4] H.E. Mynick *et al.*, Phys. Rev. Lett. **105** (2010) 095004.
[5] H.E. Mynick *et al.*, Phys. Plasmas **18** (2011) 056101.
[6] H.E. Mynick *et al.*, Plasma Phys. Control. Fusion **56** (2014) 094001.
[7] P. Xanthopoulos *et al.*, Phys. Rev. Lett. **113** (2014) 155001.
[8] D.A. Spong *et al.*, Nucl. Fusion **41** (2001) 711.
[9] J.H.E. Proll *et al.*, Phys. Rev. Lett. **108** (2012) 245002.
[10] P. Helander *et al.*, Phys. Plasmas **20** (2013) 122505.
[11] J.H.E. Proll *et al.*, Plasma Phys. Control. Fusion **58** (2016) 014006.
[12] M. Nunami *et al.*, Phys. Plasmas **20** (2013) 092307.
[13] G. G. Plunk *et al.*, Phys. Rev. Lett. 118 (2017) 105002.
[14] C. Hegna *et al.*, Physics of Plasmas **25** (2018) 022511.